AIAA 79-1660R

Instrumented Drop Tests of a Slowly Rolling Parachute Payload

V. Oskay,* W.H. Mermagen,† and J.W. Bradley‡
Ballistic Research Laboratory—ARRADCOM, Aberdeen Proving Ground, Md.

Sense and Destroy Armor (SADARM), a munition currently under development by the Army, is designed to attack an armored target from above. This munition is ejected from an artillery shell in midflight and descends to the ground while suspended from a rotating parachute. Measurements of the dynamical behavior of a model of the system were made in a series of drop tests using multisensor yawsonde instrumentation. The data were processed and analyzed using an extension of an algorithm developed originally for an artillery shell with large-amplitude yawing motions. The experimental results show that the system roll rate remains relatively constant once steady state is achieved. There are two modal frequencies in yaw and the amplitude of each mode varies throughout descent.

Nomenclature

A,B,C = coefficients of a quadratic $\phi(T)$
D,E,F = coefficients of a quadratic $\sigma(T)$
$f_k(\sigma)$ = calibrated roll angle for the kth sensor
n = number of sensors
s_k = kth sensor
t = time, ms
t_R = reference time for subset τ_5 or τ_6, ms
T = $t - t_R$, ms
$\Delta(\ )$ = $(\ ) - (\hat{\ })$
γ = sensor slit inclination with respect to canister axis, deg
θ = angular location of a sensor about canister axis with respect to an arbitrary reference line, deg
σ = solar aspect angle = the angle between the model's axis of rotation and the line of sight to the sun, deg
σ_N = complementary solar aspect angle = $90 - \sigma$, deg
τ_5 = any five consecutive times
τ_6 = any six consecutive times
ϕ = the model's roll angle in a solar fixed-plane system, deg (ϕ is measured with respect to the 2-axis in a right-handed system in which the 1-axis is along the axis of rotation and the 3-axis lies in the plane of the sun angle.)
ϕ_S = the roll angle at which a sensor sees the sun, deg
$\dot{\phi}$ = the model's roll rate in the solar fixed-plane system, rps

Superscripts

$(\hat{\ })$ = approximation to the true value of $(\ )$
$(\dot{\ })$ = $d(\ )/dt$
$(\ )'$ = $d(\ )/d\sigma$

Background

RECENT advances in millimeter-wave technology have led to the development of improved sensing munitions. STAFF (Smart Target Activated Fire and Forget) and SADARM (Sense And Destroy ARMor) systems for artillery projectiles are two such munitions presently in development. The SADARM concept is shown in Fig. 1. The system consists of a millimeter-wave radiometer and shaped-charge warhead carried by a vortex-ring parachute (VRP), suspended at a preset tilt angle to the parachute axis. The VRP is designed to impart a slow roll to the payload; the roll rate is proportional to the descent rate. Thus, the radiometer within the warhead scans a collapsing helical trace on the ground. The radiometer can distinguish between metal objects on the ground and their surroundings. If the radiometer detects a target along the helical ground trace, logic circuits associated with the device activate a firing train and a self-forging fragment is propelled toward the target.

The roll rate and yaw behavior of the SADARM system are important parameters determining the nature of the ground trace and the performance of the system. Hence a program was begun to develop methods for detecting the roll and yaw history of a SADARM model. This led to a consideration of the yawsonde.

A yawsonde is an instrument originally developed to measure the flight characteristics of artillery projectiles.[1] Since the spin of an artillery shell is an order of magnitude greater than its yaw rate, a simple yawsonde consisting of a pair of solar cells onboard the shell can be used to observe the yawing motion. The SADARM model, however, has a nominal roll rate of 5 rps and a pitch frequency of about 1 Hz. A multisensor yawsonde was required to obtain an adequate number of points during a pitch cycle. A computational algorithm for obtaining roll rates from observed data, originally proposed by Murphy[2] for large-amplitude motions, had to be extended for use with more than two sensors. Moreover, since the payload is tilted with respect to the system roll axis and performs lunar motion during descent, a method of calibration that differs from the conventional fuze-type yawsonde calibration had to be devised.

Multisensor Yawsonde

The conventional yawsonde[3] used with artillery shell has two solar cells and requires one complete revolution of the shell to determine the solar aspect angle. Fluctuations in solar aspect angle are related to the pitching and yawing motion. The usual assumptions for the two-sensor yawsonde are that neither the roll rate nor the yaw amplitude change significantly during one revolution. Since the roll rate is at least an order of magnitude greater than the yaw rate, it is possible to achieve satisfactory data density during each yaw period. The case of varying yaw during a roll period has been successfully treated by Murphy[2] and a computational method has been developed. The SADARM model, however, was expected to experience both yaw and roll rate variations during a single roll period. Moreover, if a conventional yawsonde were used, the slow roll rate of the system would result in unacceptably sparse data. Therefore, it was decided to design a multisensor yawsonde to obtain adequate yaw and roll rate measurements.

The test model was a cylindrical canister, 180 mm in diameter and 150 mm high. It was furnished with eight solar cells equally spaced about the circumference of the canister,

Presented as Paper 79-1660 at the AIAA Flight Mechanics Conference, Boulder, Colo., Aug. 6-8, 1979; submitted Nov. 26, 1979; revision received July 25, 1980. This paper is declared a work of the U.S. Government and therefore is in the public domain.

*Aerospace Engineer, Launch and Flight Division. Member AIAA.
†Physical Scientist, Launch and Flight Division. Associate Fellow AIAA.
‡Mathematician, Launch and Flight Division.

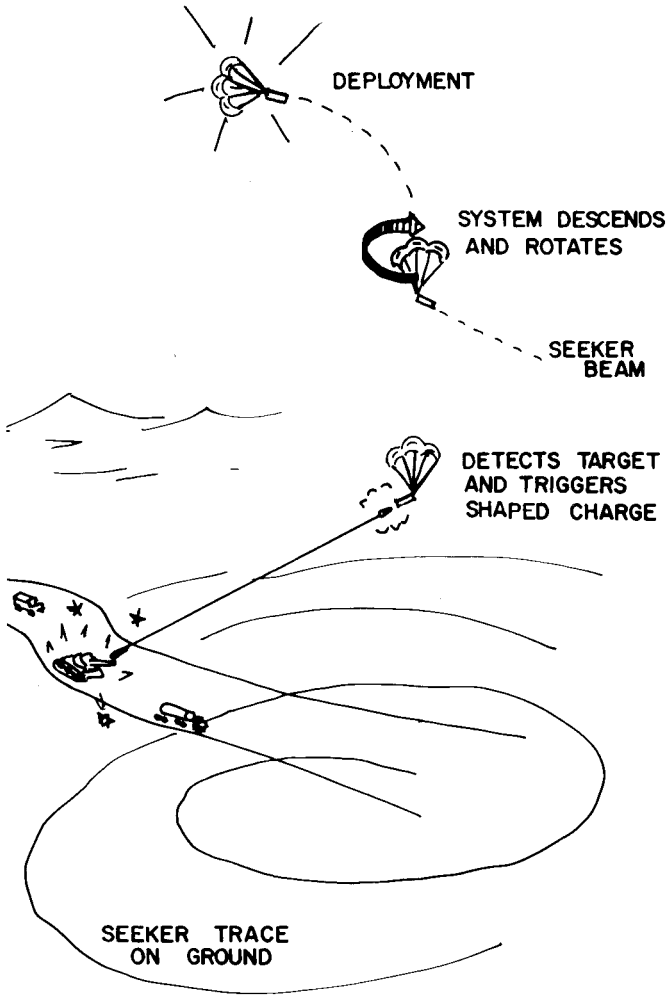

Fig. 1 SADARM employment concept.

four to measure yaw and four to measure roll rate. Important to the design of a yawsonde is the angle of inclination of each sensor slit, for this angle determines the sensitivity of the yaw measurement as well as its accuracy. In order to determine the optimum slit inclination for each sensor, it was necessary to find the functional relationship between the complementary solar aspect angle (σ_N) and the roll angle at which the sun is seen by the sensor, ϕ_S. A conceptual sketch of the instrumented SADARM model is shown in Fig. 2. From the geometry of the system, it can be shown that

$$\tan\sigma_N = A_1\cos\phi_S + A_2\sin\phi_S \tag{1}$$

where

$$A_1 = \frac{-\sin\phi\cos\theta(\sin\phi\sin\theta - \tan\gamma\cos\phi)}{(\tan\gamma\cos\phi - \sin\phi\sin\theta)\,(1-\sin^2\phi\cos^2\theta)^{1/2}}$$

$$A_2 = \frac{\cos\phi + \tan\gamma\sin\phi\sin\theta}{(\tan\gamma\cos\phi - \sin\phi\sin\theta)\,(1-\sin^2\phi\cos^2\theta)^{1/2}}$$

This rather involved expression results in a fairly simple family of curves, as is seen in Fig. 3 where σ_N is shown as a function of ϕ_S with γ as parameter. Equation (1) was used to select optimum values of γ for each sensor slit.

Pairs of sensors were coupled to voltage-controlled oscillators (VCO's) through differential amplifiers. The polarity of one sensor of each pair was inverted with respect to the other to remove ambiguity and simplify data processing. The outputs of all VCO's were combined in a mixer-amplifier and the composite signal modulated an L-band transmitter. Figure 4 shows the circuit for the eight-sensor unit in block diagram form. The transmitter was

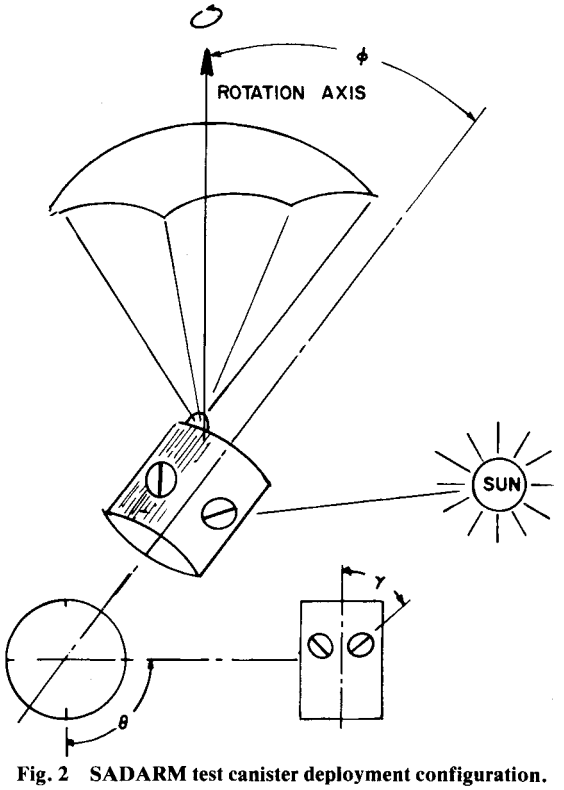

Fig. 2 SADARM test canister deployment configuration.

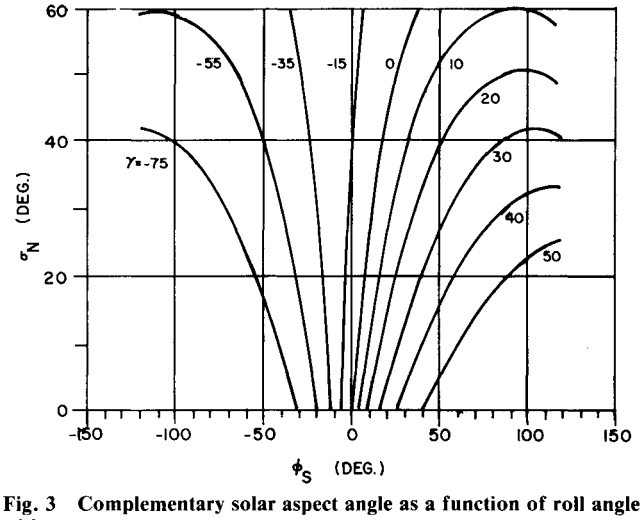

Fig. 3 Complementary solar aspect angle as a function of roll angle with γ as parameter.

coupled to a scimitar antenna located at the top of the canister. The components inside the canister were potted with polyurethane foam to protect against impact while permitting easy removal of components for repair. The antenna was designed to be replaceable.

In order to compute the yawing behavior of a model from the yawsonde data, a calibration must be performed to determine ϕ_S as a function of σ_N for each sensor. For the SADARM model, the conventional yawsonde calibration technique[4] had to be modified to allow for the system's lunar motion. The resulting calibration curves for the yaw sensors are shown in Fig. 5 with ϕ_S plotted as a function of σ_N.

Drop Tests

The test program was designed to determine the model's dynamic behavior under canyon and helicopter drop environments. The canyon environment was important since a live demonstration test was scheduled for a later date. On the other hand, the helicopter drops were to provide dynamic data

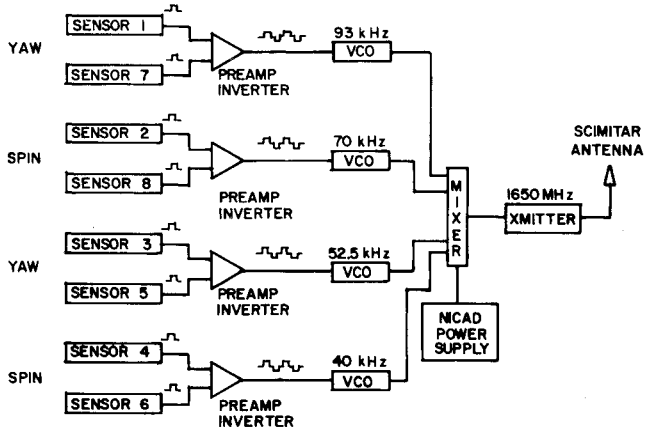

Fig. 4 Eight-sensor SADARM electronics for motion measurements.

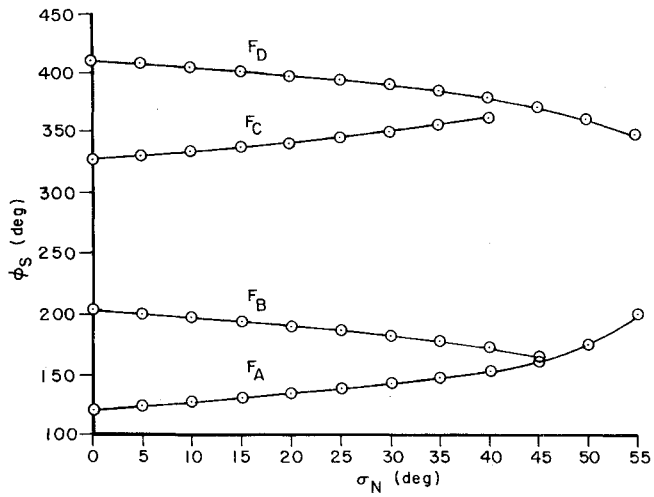

Fig. 5 Calibration curves for yaw sensors, where $F_k = F_k(\sigma)$.

under long-duration steady-state conditions. The effect of VRP diameter on the model's dynamic behavior was also studied during these tests.

The 180 mm model weighed 15.6 kg with transverse and polar moments of inertia of 0.105 and 0.104 kg-m^2, respectively. These almost-equal moments of inertia made the payload behave as a spheroid of inertia with no preferred major axis. Two VRP's were tested with diameters of 1.83 and 2.13 m, the larger parachute being the decelerator of primary interest. During the cable drop tests into the canyon, the parachutes were predeployed to minimize the effects of canyon environment during unfurling. During the helicopter tests, the parachutes were contained in a bag below the helicopter prior to release.

The yawsonde data were transmitted via L-band through an FM-FM link. The video signal from the transmitter was recorded on an analog tape together with the range time signal, which could later be used to correlate yawsonde results with other data. The position of the model during a drop was measured with a laser tracker which produced a digital printout of slant range, altitude, and descent velocity as a function of drop time. A documentary movie camera was slaved to the laser tracker.

Data Reduction

The raw flight data consist of a series of analog pulses from each solar sensor as it sees the sun, recorded vs range time. The problem is to compute the roll angle (ϕ) and complementary solar aspect angle (σ_N) histories, given the in-flight times for each sensor and the corresponding calibration curves, Fig. 5.

We label the four yaw sensors in alphabetical order (S_A, S_B, S_C, and S_D) as they are encountered when proceeding around the canister in the direction of positive roll.

For each sensor, we can define the roll angle as some convenient differentiable function of the sun angle, involving unknown parameters. The laboratory calibrations enable us to evaluate these parameters, say by a least-squares fit. For sensor S_A, let f_A be the function determined in this manner, so that $f_A(\sigma)$ is our approximation to the calibrated roll angle at a specified sun angle σ. Similarly, we determine f_B, f_C, and f_D. It should be noted that the roll angle measurements necessarily fall between 0 and 360 deg. However, in anticipation of a positive roll rate, we make sure – by suitable 360-deg additions to the raw S_C and S_D data – that the roll angle values increase from S_A to S_B to S_C to S_D. That is, for any σ in the anticipated flight range, we have

$$f_A(\sigma) < f_B(\sigma) < f_C(\sigma) < f_D(\sigma) < 2\pi + f_A(\sigma) \tag{2}$$

Flight data yield four sets of times:

$$t_1 < t_5 < t_9 \ldots . \text{ from sensor } S_A$$

$$t_2 < t_6 < t_{10} \ldots . \text{from sensor } S_B$$

$$t_3 < t_7 < t_{11} \ldots . \text{from sensor } S_C$$

$$t_4 < t_8 < t_{12} \ldots . \text{from sensor } S_D$$

From many drops, the intermingled times increased without exception:

$$t_1 < t_2 < t_3 < t_4 < t_5 \ldots . \tag{3}$$

but this is not always the case.

Murphy considered the behavior of the system over a subset of five consecutive times; for convenience, we denote any such subset as τ_5. He assumed that over the subset τ_5, σ is linear and ϕ is quadratic in time. Alternatively, we could consider σ quadratic and ϕ linear over τ_5 or we could consider both σ and ϕ quadratic in time over a subset τ_6 of six consecutive times. We present here the six-parameter approach. That is, over each subset τ_6, we assume that

$$\phi = A + B \cdot T + C \cdot T^2 \qquad \sigma = D + E \cdot T + F \cdot T^2 \tag{4}$$

where (A,B,C,D,E,F) are unknown constants (whose values change, of course, with the subset τ_6), where $T = t - t_R$ and where t_R is a known reference time (say, the average of the first and last times) for each subset τ_6.

Murphy presented his algorithm for two sensors; here we assume four. The generalization to n sensors is straightforward. For n sensors, τ_5 and τ_6 encompass $5/n$ and $6/n$ roll periods, respectively. Hence the greater the number of sensors, the more acceptable are the assumptions of Eqs. (4) over a subset.

If we can determine σ at some time t_i associated with sensor S_k $(k = A,B,C,D)$, then we know the roll angle at that time to within a multiple of 2π:

$$\phi(t_i) = f_k(\sigma(t_i)) + 2\pi j \tag{5}$$

We can rewrite Eq. (5) as

$$\phi_i = f_k(\hat{\sigma}_i + \Delta\sigma_i) + 2\pi j \tag{6}$$

where ($\hat{}$) denotes an approximation to the true value. The basic equation of the algorithm is simply the first-order Taylor expansion of Eq. (6):

$$\phi_i = f_k(\hat{\sigma}_i) + f_k'(\hat{\sigma}_i) \cdot \Delta\sigma_i + 2\pi j \tag{7}$$

where the prime denotes differentiation with respect to σ.

For a specified subset τ_6, Eqs. (4) allow us to rewrite Eq. (7) in the form

$$A+B\cdot T_i+C\cdot T_i^2-f_k'(\hat{\sigma}_i)\,[\Delta D+T_i\cdot\Delta E+T_i^2\Delta F]=f_k(\hat{\sigma}_i)+2\pi j \tag{8}$$

where

$$\hat{\sigma}_i=\hat{D}+\hat{E}\cdot T_i+\hat{F}\cdot T_i^2 \tag{9}$$

Thus if we can obtain initial estimates $\hat{D}_0,\hat{E}_0,\hat{F}_0$ and hence $\hat{\sigma}_{i0}$, Eq. (8) contains six unknowns: $(A,B,C,\Delta D,\Delta E,\Delta F)$. The six times of subset τ_6, when substituted in Eq. (8), provide us with the six equations needed to solve for the six unknowns.

The multiples of 2π in Eq. (8) are easily determined for any subset by the requirement that throughout that subset the right-hand sides of Eq. (8) should increase with time. Since inequality (2) ensures this increase for an (S_A,S_B,S_C,S_D) cycle, it is sufficient to add or subtract 2π for any adjoining cycles. For example, if the six times of subset τ_6 correspond to sensors $(S_D,S_A,S_B,S_C,S_D,S_A)$, then the term $2\pi j$ in Eq. (8) becomes $(-2\pi,0,0,0,0,2\pi)$ for the six equations.

Once we have obtained the increments ΔD, ΔE, and ΔF, we can update the parameter estimates $\hat{D},\hat{E}$, and $\hat{F}$:

$$\hat{D}_1=\hat{D}_0+\Delta D \qquad \hat{E}_1=\hat{E}_0+\Delta E \qquad \hat{F}_1=\hat{F}_0+\Delta F \tag{10}$$

and hence we can update the sun angle values $\hat{\sigma}_i$ at the six times. These values are substituted back in the system of Eq. (8), which is solved again for the six unknowns, and so on. This iterative process usually converges (that is, the increments $\Delta D,\Delta E,\Delta F$ become satisfactorily small) in a few iterations. The desired final results for the subset are the final values of B (the roll rate at the reference time for the subset) and D (the corresponding sun angle).

We can now move along the set of times to our next selected subset τ_6 and repeat the entire process. Our first subset consists of times t_1 to t_6 from sensors S_A,S_B,S_C,S_D,S_A,S_B. If we choose a time step of 1, our next subset is t_2 to t_7, corresponding to sensors S_B,S_C,S_D,S_A,S_B,S_C. Again, we need initial estimates $\hat{D}_0,\hat{E}_0,\hat{F}_0$. We found that for each subset τ_6, we could take $\hat{E}_0$ and $\hat{F}_0$ as zero and for each subset after the first, we could set $\hat{D}_0$ equal to the final D of the previous subset.

Proceeding in this manner over the entire time set, we obtain the desired roll rate and sun angle histories.

Results

In general, the payload instrumentation worked as designed. Some periodic noise observed in the data has been attributed to radio-frequency interference from the mechanical linkage between parachute and model. This linkage consists of a slip-coupling to limit the torque transmitted from the VRP to the model in order to prevent twisting of the parachute lines. During the test program, an abundance of data was produced. Only representative samples will be presented to indicate the overall system behavior. The test data will be discussed in two groups. First, we will discuss the spin behavior of the system under various test conditions. The data are presented as plots of $\dot{\phi}$ vs time. Second, the yawing behavior of the instrumented models will be shown as plots of σ_N vs drop time.

The roll behavior of cable drop 7 is shown in Fig. 6. This drop was made with a 2.13 m VRP. No data are available until 3 s into the drop, at which time the VRP developed sufficient torque to drive the system. Steady-state spin of about 4.7 rps is achieved at 4 s. The $\dot{\phi}$ data show periodic modulations of the steady-state roll. The singular feature of these oscillations is that they occur at the average spin rate. The amplitude of the oscillations remains relatively constant for the entire drop.

The roll history for helicopter drop 10 at the beginning of its flight is plotted in Fig. 7. The model used a 2.13 m parachute and was released at an altitude of 915 m. About 50 s of yawsonde data were obtained. The roll data do not start until 3.5 s into the drop and then reach a steady-state value of 4.7 rps within the next second. The same high-frequency modulation is present in this plot although it is not as prevalent as in Fig. 6. In addition, there appears to be a low-frequency modulation.

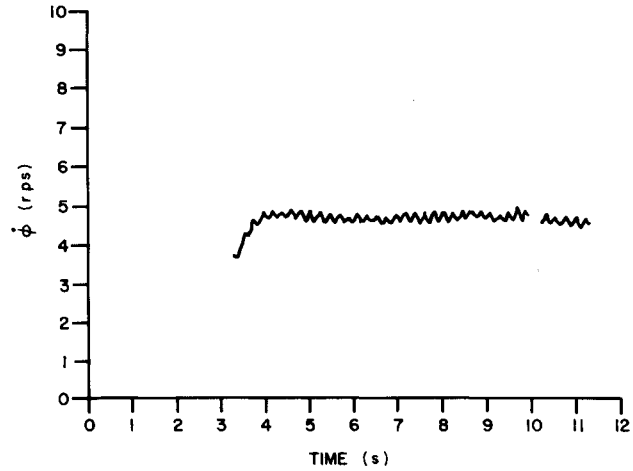

Fig. 6 Spin history of cable drop 7.

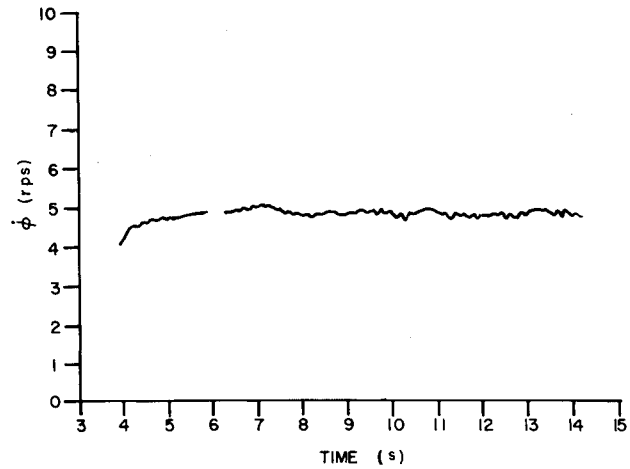

Fig. 7 Spin history, 4-14 s, for helicopter drop 10.

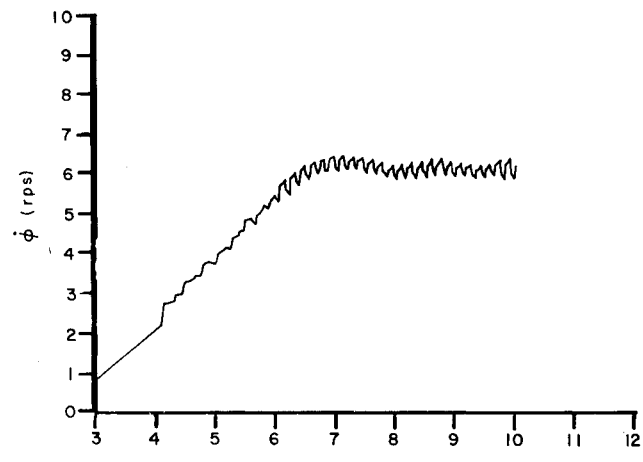

Fig. 8 Spin vs time for cable drop 18.

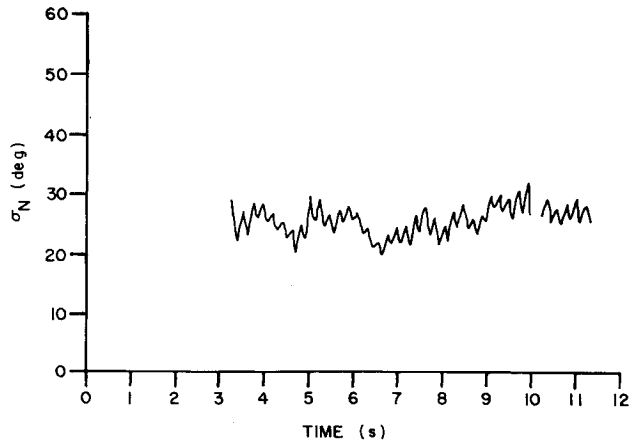

Fig. 9 Aspect angle history for cable drop 7.

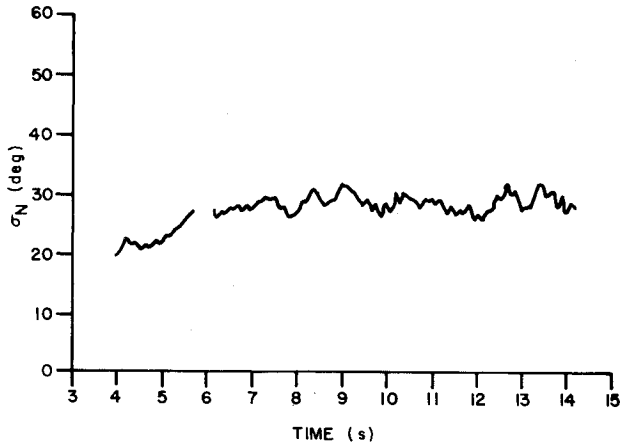

Fig. 10 Aspect angle, 4-14 s, for helicopter drop 10.

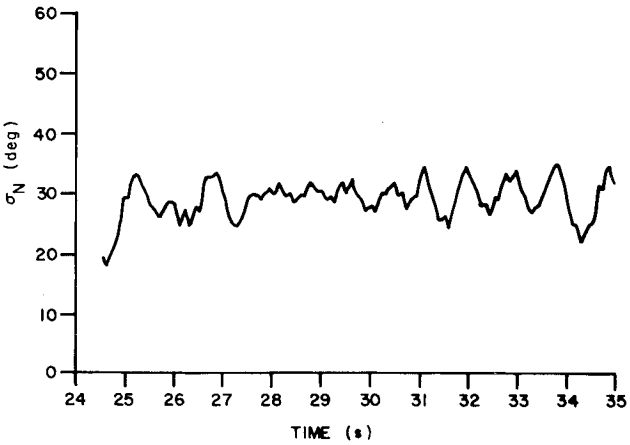

Fig. 11 Aspect angle, 24-35 s, for helicopter drop 10.

An example of the roll history from a cable drop using the smaller, 1.83 m, VRP is shown in Fig. 8. Again, the data do not start until 3 s into the drop. The transition time for the smaller parachute is about 3.5 s and the steady-state value is about 6 rps. The high-frequency modulation of the average $\dot{\phi}$ is obvious although now the frequency is about 6 Hz.

The yaw history of the cable drop with 2.13 m VRP, drop 7, is shown in Fig. 9. The data indicate that the system has a bimodal yawing behavior. The fast rate is at the same frequency as the average steady-state roll rate while the slow frequency, between 0.5 and 1.0 Hz, is near the pendular frequency of the system. A similar behavior was observed for the cable drops using the smaller parachute, although in those cases the frequency of the fast rate was about 6 Hz, which was the average roll rate for those drops.

The partial yawing history for a helicopter drop with the large parachute is shown in Figs. 10 and 11. The bimodal nature of the system is still observable in these figures, although the amplitude of the fast mode is somewhat less than for the corresponding cable drop, Fig. 9. On the other hand, the amplitude of the slow mode varies considerably, reaching peak-to-peak amplitudes of 12 deg at certain portions of the drop.

Discussion

Compared to an earlier test program with a similar design,[5] these tests showed some interesting and unexpected flight behavior. Most of the yaw histories showed a bimodal motion with the fast frequency at the average steady-state spin rate of the system. This was true for both cable and helicopter drops and both parachute sizes. The spin histories also showed the presence of the same fast frequency. The experimental concern centered on the question of whether these oscillations were real, and, if they were, whether the yawsonde could adequately measure a yawing mode that has the same frequency as the system's spin rate. Exact test cases were generated[6] and analyzed using the computational algorithm described earlier. These test cases generated bimodal motions at or near the spin rate of the system. The algorithm was capable of reducing the test case amplitude data with an accuracy of about 50% for the case where the spin rate and the yaw rate were exactly equal. When the spin rate was five times the pitch rate, the reduced data were accurate to within 5% of the test case inputs. The conclusion is that the modal frequencies shown in the yawsonde data appear to be correct. The amplitudes may be low.

Since the roll-producing torque of a VRP depends on the dynamic pressure, a finite time is required for the system to achieve steady-state spin. In all cases, however, the system had attained steady state by 4 s into the drop if a 2.13 m VRP was used. For a 1.83 m parachute, the transitional period was approximately 3 s longer. The slow mode appears to be excited by wind gusts, and its frequency is that of the system acting as a pendulum. The fast-frequency yawing mode is presumably excited by the interaction between the parachute and the model through the friction coupler. It is believed that the deviation of the model physicals from those of a perfect spheroid of inertia may be the cause of the fast mode. At present, no physical model has been developed to explain the unusual motion observed.

Conclusions

We have shown that the extended version of the yawsonde reduction algorithm, originally developed by Murphy, is capable of producing yaw and spin histories for slowly rolling models instrumented with multisensor yawsondes. The computer program is currently capable of handling any combination of sensors up to a total of eight. The method has been proven to be flexible enough to obtain yaw histories where one of the modal frequencies is close to the spin rate of the system.

Instrumented models tested during this program have shown interesting dynamic behavior. Although the most important aspect of the model's behavior is the ground path traced by the canister's axis of symmetry (which would correspond to the detector axis), at present no method exists to translate the model's yaw history to a ground trace due to the lack of a theoretical model for the dynamic characteristics of this test vehicle. Further work in this area is important.

It would also be of interest to test a multisensor instrumented model with other types of decelerators, such as guide-surface-rotor parachutes, ballutes, or even non-parachute type decelerators. These experiments may answer the question whether the bimodal behavior of the system is caused solely by the present components or is inherently due to a model designed as an imperfect spheroid of inertia.

Acknowledgments

The consultation and assistance of R. Kline, T. Hoffman, and D. Griggs of the Large Caliber Weapon Systems Laboratory, ARRADCOM, in the application of the vortex-ring parachute merit recognition. The cooperation of the personnel of Sandia Laboratories during the test phase of the program is gratefully acknowledged.

References

[1]Mermagen, W.H., "Measurements of the Dynamical Behavior of Projectiles over Long Flight Paths," *Journal of Spacecraft and Rockets,* Vol. 8, April 1971, pp. 380-385.

[2]Murphy, C.H., "Effect of Large High-Frequency Angular Motion of a Shell on the Analysis of Its Yawsonde Records," Ballistic Research Laboratory, Aberdeen Proving Ground, Md., BRL Memorandum Rept. 2581, Feb. 1976.

[3]Mermagen, W.H. and Clay, W.H., "The Design of a Second Generation Yawsonde," Ballistic Research Laboratory, Aberdeen Proving Ground, Md., BRL Memorandum Rept. 2368, April 1974.

[4]Clay, W.H., "A Precision Yawsonde Calibration Technique," Ballistic Research Laboratory, Aberdeen Proving Ground, Md., BRL Memorandum Rept. 2263, Jan. 1973.

[5]Mermagen, W.H., Oskay, V., and Bradley, J.W., "Yawsonde Tests of SADARM Warhead at Sol Se Mete Canyon, Albuquerque, New Mexico," Ballistic Research Laboratory, Aberdeen Proving Ground, Md., ARBRL-MR-02918, May 1979.

[6]Oskay, V. and Mermagen, W.H., "Helicopter and Cable Drop Tests of a Multi-Sensor Yawsonde Instrumented SADARM Model," Ballistic Research Laboratory, Aberdeen Proving Ground, Md., BRL memorandum report in process.